Препринти Інституту фізики конденсованих систем НАН України розповсюджуються серед наукових та інформаційних установ. Вони також доступні по електронній комп'ютерній мережі на WWW-сервері інституту за адресою http://www.icmp.lviv.ua/

The preprints of the Institute for Condensed Matter Physics of the National Academy of Sciences of Ukraine are distributed to scientific and informational institutions. They also are available by computer network from Institute's WWW server (http://www.icmp.lviv.ua/)

Микола Володимирович Максименко
Андреас Гонекер
Рьодріх Мьоснер
Йоганнес Ріхтер
Олег Володимирович Держко

Феромагнітний перехід у плоскозонній моделі Габбарда як перколяційний перехід за наявності кореляцій через принцип Паулі

Роботу отримано 26 грудня 2011 р.

Затверджено до друку Вченою радою ІФКС НАН України

Рекомендовано до друку відділом теорії модельних спінових систем

Виготовлено при ІФКС НАН України

Національна академія наук України

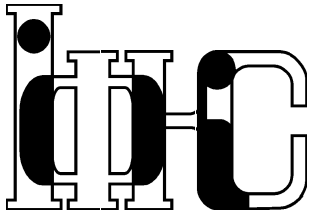

ІНСТИТУТ ФІЗИКИ КОНДЕНСОВАНИХ СИСТЕМ

ICMP–11–14E

M.Maksymenko, A.Honecker[*], R.Moessner[†], J.Richter[‡], O.Derzhko

THE FLAT-BAND FERROMAGNETIC TRANSITION AS A PAULI-CORRELATED PERCOLATION TRANSITION

[*]Institut für Theoretische Physik, Georg-August-Universität Göttingen, Friedrich-Hund-Platz 1, 37077 Göttingen, Germany
[†]Max-Planck-Institut für Physik Komplexer Systeme, Nöthnitzer Straße 38, 01187 Dresden, Germany
[‡]Institut für Theoretische Physik, Universität Magdeburg, P.O. Box 4120, 39016 Magdeburg, Germany

ЛЬВІВ

УДК: 537.9; 537.622

PACS: 71.10.-w

Феромагнітний перехід у плоскозонній моделі Габбарда як перколяційний перехід за наявності кореляцій через принцип Паулі

М.Максименко, А.Гонекер, Р.Мьоснер, Й.Ріхтер, О.Держко

Анотація. Розглянувши модель Тасакі-Габбарда на квадратній гратці, ми показали, що вона має феромагнітні основні стани при концентрації електронів $0.22\ldots \leq n/N \leq 1/3$.

The flat-band ferromagnetic transition as a Pauli-correlated percolation transition

M.Maksymenko, A.Honecker, R.Moessner, J.Richter, O.Derzhko

Abstract. Considering the square-lattice Tasaki-Hubbard model we have shown that it has ferromagnetic ground states for the electron concentration $0.22\ldots \leq n/N \leq 1/3$.

Подається в Physical Review Letters
Submitted to Physical Review Letters

It is known that flat bands yield a route to ferromagnetism in the Hubbard model, but the actual location and nature of the para-ferro transition remain unknown. We study the N-site Hubbard model on the 2D Tasaki lattice. For electron densities $n \leq \mathcal{N} = N/3$, many-electron ground states can be constructed from one-particle states localized in trapping cells. If electrons in neighboring traps are in a symmetric spin state, due to the Pauli principle on-site repulsion is not active, i.e., electrons can form a ferromagnetic cluster. Ground-state ferromagnetism can be analyzed as a new Pauli-correlated site-percolation problem on the square lattice, where due to the degeneracy of independent ferromagnetic clusters different cluster coverings of electrons obtain different weights. We provide an exact solution for the corresponding 1D case and a numerical algorithm for the 2D case of the new percolation problem. In 2D the para-ferro transition takes place at concentration $p = n/\mathcal{N} = p_f = 0.66 \pm 0.01$ that is well above the threshold for the standard site percolation on the square lattice $p_c \approx 0.59$. Moreover, there exists a region above p_f where ferromagnetism appears unsaturated.

1. Introduction

The interplay of the Coulomb interaction with the Pauli principle was already recognized by Heisenberg [1] to give rise to a ferromagnetic exchange interaction, also encoded in Hund's rule about aligned spins in a partially filled shell. For a many-body system of correlated electrons with a flat band, when the interaction energy completely dominates over the kinetic energy, the ferromagnetic instability is one of the few problems for which exact results are available, albeit for a restricted range of fillings.

Given the renewed interest in correlation effects in flat-band systems [2], here we provide a detailed analysis of a flat-band ferromagnet with an on-site Hubbard interaction of strength $U \geq 0$. For lattices with a flat band, for $U = 0$, any state involving electrons occupying the flat band only is trivially a ground state. Crucially, this degeneracy is only partially lifted when a repulsive $U > 0$ is switched on. The basic reason is that the Pauli principle, by demanding an antisymmetric pair wavefunction, makes the overlap between two electrons on the same site vanish provided they are in a symmetric spin state. As the density of electrons increases, ferromagnetic clusters of increasing size appear. The degeneracy, $n+1$, of a ferromagnetic cluster containing n electrons, gives differing weights to different clustering of electrons. The ferromagnetic transition corresponds to the emergence of a cluster containing a nonzero fraction

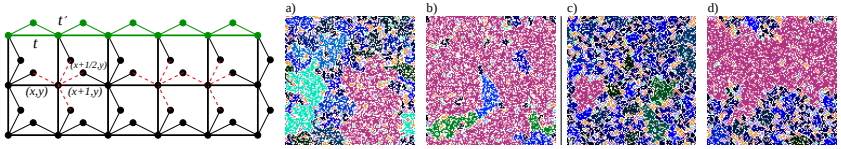

Figure 1. (Color online) Two-dimensional Tasaki lattice [hopping integrals t (thick lines) and t' (thins lines)] and snapshots of configurations for standard and Pauli-correlated percolation for deviations 3% from critical concentration. A trapping cell contains five sites (dashed red lines). The green circles and lines show the 1D variant of the lattice (sawtooth chain). Panels a) and b) show snapshots (lattice extension $\mathcal{L} = 120$) of configurations for standard percolation for concentrations $p_1 = 0.574$ and $p_2 = 0.609$ ($p_c = 0.592746$), while panels c) and d) show snapshots for Pauli-correlated percolation for $p_1^* = 0.64$ and $p_2^* = 0.68$ (here we assume $p_f = 0.66$). Here open boundary conditions along the vertical axis are implemented to illustrate the effect of the weights.

of the electrons.

An early remark by Mielke [3] likened this problem to one of percolation. Mielke and Tasaki [4] later remarked that, for a class of flat-band ferromagnets on particularly decorated lattices, the percolation problem in question is not a standard one but rather one including non-trivial weights.

Here, we develop this analogy in detail. First of all, we point out that the interaction between the clusters, on account of its 'statistical origin' in the Pauli principle, is unusual in that it is range-free and purely geometric – two particles interact only if they form part of the same cluster. The interaction is not pairwise either but only depends on the size of the cluster, even being irrespective of the shape of the cluster. Despite its long range, the statistical interaction does saturate.

This motivates the study of an unusual percolation problem, which we call Pauli-correlated percolation, which we find has a number of interesting features in its own right. It provides an instance of a problem in the quantum physics of strongly correlated electrons which can be 'reduced' to a highly non-trivial problem in classical statistical mechanics, on which an entirely different set of tools can be brought to bear. We first demonstrate some special features of this problem by providing a complete exact solution to a one-dimensional (1D) version of this model, which exhibits a tendency to breaking up large clusters as well as a

development of spatial correlations.

For the two-dimensional (2D) Tasaki lattice (see Fig. 1), a decorated square lattice, we provide an analysis of its phase diagram and critical properties. Using a numerical algorithm custom-tailored to the problem at hand by extending the Hoshen-Kopelman and Newman-Ziff algorithms [5, 6] for standard percolation, we establish that the ferromagnetic transition does indeed take place in the form of a percolation transition at a filling $p_f = 0.66 \pm 0.01$ comfortably in excess of the corresponding well-known percolation transition on the square lattice at $p_c = 0.5927460\ldots$ [7].

We show that the transition is either continuous or at most weakly first order. In particular, the probability of encountering a spanning cluster does not jump discontinuously from 0 to 1 at p_f, in distinction to standard percolation. This observation is of a piece with the appearance of an extended regime of unsaturated ferromagnetism as a function of density.

The remainder of the paper is organized as follows. First, we introduce and define the problem at hand. Following the exact solution of the 1D problem, we briefly describe our algorithm and summarize the central numerical findings, both from a quantum magnetic and classical percolation perspective. We back up these claims by providing an exact diagonalization study of a finite-size system. Finally, we close by pointing out open questions and directions for future research.

2. Percolation representation

We consider the Hubbard model

$$H = \sum_{\sigma=\uparrow,\downarrow} \sum_{\langle i,j \rangle} t_{i,j} \left(c_{i,\sigma}^{\dagger} c_{j,\sigma} + \text{h.c.} \right) + U \sum_{i} n_{i,\uparrow} n_{i,\downarrow} \tag{2.1}$$

with standard notations. As a representative for a 2D flat-band system we consider the Tasaki lattice [4] shown in Fig. 1, although our approach, in principle, can be adapted to other flat-band lattices. Note that Tasaki's lattice decoration [4] can be used also for other lattices. Moreover, it can be performed in arbitrary dimension by a corresponding decoration of each bond of a D-dimensional lattice. This allows a direct comparison of the 1D and the 2D problem. We assume that the two relevant hopping integrals obey the relation $t' = \sqrt{z}t > 0$, where z is the coordination number z of underlying lattice. Then the lowest-energy one-electron band of the Tasaki lattice is completely dispersionless (flat) and the corresponding set of one-electron states can be taken as localized on trapping cells.

In $D = 2$ each trapping cell consists of one site of the underlying square lattice and four neighboring decorating sites (cf. Fig. 1) therefore z=4. A localized eigenstate of energy $\varepsilon_1 = -zt = -4t$ of an electron with spin σ is given by $l^\dagger_{\mathbf{r},\sigma}|0\rangle$, where $\mathbf{r} = x, y$ runs over the sites of the underlying square lattice, $l^\dagger_{\mathbf{r},\sigma} = c^\dagger_{x-\frac{1}{2},y,\sigma} + c^\dagger_{x+\frac{1}{2},y,\sigma} + c^\dagger_{x,y-\frac{1}{2},\sigma} + c^\dagger_{x,y+\frac{1}{2},\sigma} - 2c^\dagger_{x,y,\sigma}$, and $|0\rangle$ denotes the vacuum state. Localized many-particle ground states for $n > 1$ electrons with energy $n\varepsilon_1$ are constructed by filling the traps with the electrons avoiding double occupancy of a cell and taking into account the Pauli principle which is crucial if electrons occupy neighboring cells: If m electrons occupy m contiguous traps (i.e., build a connected cluster), the m electrons must be in a symmetric spin state, i.e., in one of the $m+1$ spin-$m/2$ multiplet states. The maximum filling with localized electrons is $n_{\max} = \mathcal{N} = N/3$, where $\mathcal{N}$ is the number of cells (number of sites of the underlying square lattice). The ground state of n electrons, $n \le \mathcal{N}$, has a huge degeneracy

$$g_{\mathcal{N}}(n) = \sum_{q=1}^{\mathcal{C}^n_{\mathcal{N}}} W(q), \quad W(q) = \prod_{i=1}^{M_q} (n_{q;i} + 1). \tag{2.2}$$

Here q enumerates possible geometrical configurations of n electrons on $\mathcal{N}$ cells. For a particular spatial configuration q, M_q denotes the number of separated clusters having $n_{q;i}$ electrons, $i = 1, \ldots, M_q$, $\sum_{i=1}^{M_q} n_{q;i} = n$.

Comparing the prediction obtained by this localized-state picture with exact diagonalization results for the full energy spectrum of the Hubbard model for finite Tasaki lattices, we found numerical evidence for completeness of the set of localized states for the Tasaki-Hubbard model. Moreover, for finite systems this set is linearly independent and separated from higher-energy states by a finite gap.

The emergent geometrical visualization of the ground states combined with percolation analysis becomes extremely useful for examining the transition to a ferromagnetic ground state. If the electron concentration $p = n/\mathcal{N}$ exceeds a critical value, a percolating cluster appears that contains a finite fraction of electrons, giving rise to a finite value of the averaged square of the total spin $\langle \mathbf{S}^2 \rangle / \mathcal{N}^2$ [3, 4]. For $\langle \mathbf{S}^2 \rangle$ we can write

$$\begin{aligned} \langle \mathbf{S}^2 \rangle &= \frac{1}{g_{\mathcal{N}}(n)} \sum_{q=1}^{\mathcal{C}^n_{\mathcal{N}}} W(q) \sum_{i=1}^{M_q} \frac{n_{q;i}}{2} \left(\frac{n_{q;i}}{2} + 1 \right) \\ &= \sum_{l=1}^{n} \mathcal{N} n(l) \frac{l}{2} \left(\frac{l}{2} + 1 \right), \end{aligned} \tag{2.3}$$

where we have introduced the averaged number of clusters of size l (normalized by the lattice size $\mathcal{N}$) [7],

$$n(l) = \frac{1}{g_{\mathcal{N}}(n)} \sum_{q=1}^{\mathcal{C}^n_{\mathcal{N}}} W(q) n_q(l) \tag{2.4}$$

with $n_q(l)$ denoting the number of clusters of size l for a particular geometric configuration q.

It is in order to emphasize here the important difference between the Pauli-correlated percolation and the standard one. The number of clusters of size l is given also by Eq. (2.4), however, in the latter case with $g_{\mathcal{N}}(n) = \mathcal{C}^n_{\mathcal{N}}$ and $W(q) = 1$. The weight factor $W(q)$ arising owing to the degeneracy of ferromagnetic clusters has a tremendous effect on the percolation, changing the percolation threshold, the spanning probability, the normalized cluster number etc. These differences are also obvious in snapshots of typical configurations for standard and Pauli-correlated percolation at concentrations slightly below and above the transition point, see Fig. 1. Before we shall illustrate this for the 2D model in more detail, we first present the exact solution for the 1D Tasaki-Hubbard model (i.e., the Hubbard model on the sawtooth chain) [4, 8] as a 1D percolation problem.

3. Exactly solvable Tasaki chain

We use the transfer-matrix method [9] to solve the 1D Pauli-correlated percolation problem. The population of traps (V-shaped valleys) on the $2\mathcal{N}$-site sawtooth chain by n electrons in accordance with the Pauli principle is encoded in 3×3 transfer matrix (see the Appendix). In the limit $\mathcal{N} \to \infty$,

$$n(l) = \frac{4(1-p)^3}{(2-p)^2} (l+1) \alpha^l \ , \ \alpha = \frac{p}{2-p}. \tag{3.1}$$

$n(l)$ has a maximum at $l^\star = -(1 + 1/\ln \alpha)$, where $l^\star > 1$ for $p > 2/(\sqrt{e}+1) \approx 0.755$. Eq. (3.1) is significantly different from the standard percolation result $n(l) = (1-p)^2 p^l$ [7], that leads to $l^\star = 1$ independent of p. Only for small p both cases are similar. The combination of Eqs. (3.1) and (2.3) yields

$$\langle \mathbf{S}^2 \rangle = \frac{3p(2-p)}{8(1-p)} \mathcal{N}. \tag{3.2}$$

Hence, the magnetic moment $\langle \mathbf{S}^2 \rangle / \mathcal{N}^2$ tends to zero for $p < 1$, i.e., the percolation threshold is $p_f = 1$. This rigorous conclusion found for

$\mathcal{N} \to \infty$ is in accordance with previous findings [8], however obtained there not in a rigorous way.

Finally we use the transfer-matrix approach to calculate the (pair) site-occupation correlation function $g(|i-j|) = \langle n_i n_j \rangle - \langle n_i \rangle \langle n_j \rangle$ [10]. Our result reads: $g(|i-j|) = -(1-p)^2 e^{-|i-j|/\xi} < 0$ with $\xi = -1/(2\ln\alpha)$. ξ diverges as $(p_f - p)^{-1}$ when $p \to p_f = 1$ and $g(|i-j|)$ becomes long ranged and weak. This should be contrasted to standard percolation where $g(|i-j|) = p(1-p)\delta_{i,j}$. Clearly, the Pauli correlated percolation leads to an effective repulsive force.

Our findings for the 1D case also lead to the conclusion that the considered system prefers to form as many small clusters as possible instead of one (or a few) large cluster(s). Such spatial configurations are favored due to the weight factor $W(q)$. This effect, however, is much less pronounced for $D = 2$, to which we turn next.

4. Transition to ferromagnetic ground states in two dimensions

Although for the 2D case we have no analytical solution, some basic features of the Pauli-correlated percolation remain. We examine the 2D Pauli-correlated percolation numerically. In contrast to the standard percolation, simple random sampling of geometrical configurations is not sufficient for averaging in our case, since various geometrical configurations have different weights $W(q)$. Going beyond standard numerical schemes [5, 6], to take into account efficiently various geometrical configurations according to their weights, we have implemented importance sampling choosing samples according to the distribution of $W(q)$. For a fixed number of electrons, we generate a new configuration q_2 from the given one q_1 by a random permutation of two sites accepting the new configuration with probability $\min[1, W(q_2)/W(q_1)]$ (Metropolis algorithm). As a result, the numerical investigation of the Pauli correlated percolation becomes more challenging, since it suffers from critical slowing down (that does not occur in standard-percolation simulations). Labeling of clusters is done in two different ways: 1) using a modified Newman-Ziff algorithm [6] which locally updates cluster labeling for fixed number of occupied sites and 2) using the Hoshen-Kopelman algorithm [5] which makes a global update. Our main findings concern $\langle \mathbf{S}^2 \rangle$, the spanning probability P_{span}, and $n(l)$, see Figs. 2 and 3.

First we discuss the magnetic moment of the largest cluster $M^2 = \langle \mathbf{S}^2_{\text{maxcluster}} \rangle / \mathbf{S}^2_{\text{max}}$, $\mathbf{S}^2_{\text{max}} = (n/2)(n/2+1)$. $M^2 > 0$ indicates the appearance of a ferromagnetic cluster proportional to the system size which

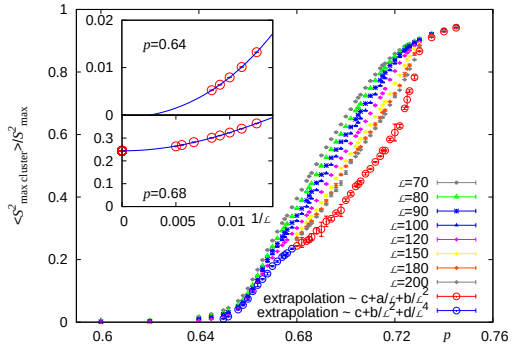

Figure 2. (Color online) Square of the magnetic moment of the largest cluster $M^2 = \langle \mathbf{S}^2_{\text{maxcluster}} \rangle / \mathbf{S}^2_{\text{max}}$ versus $p = n/\mathcal{N}$ for the 2D Tasaki lattice. Inset: Finite-size scaling of M^2 at $p = 0.64$ and $p = 0.68$.

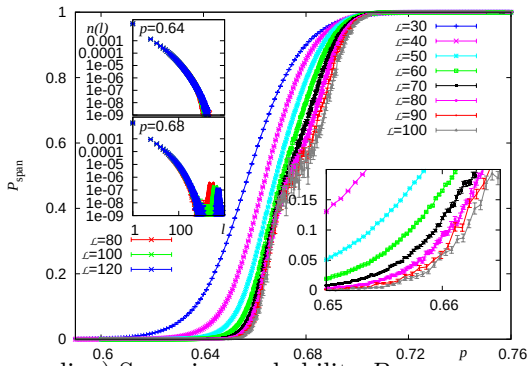

Figure 3. (Color online) Spanning probability P_{span} versus $p = n/\mathcal{N}$ and inset with magnification of the region near p_f. Left inset: Normalized number of clusters $n(l)$ at $p = 0.64$ and $p = 0.68$ for $\mathcal{L} = 80,\ 100,\ 120$.

dominates the macroscopic magnetic response of the system [4]. We have calculated M^2 for finite systems up to 250×250 sites implying both periodic and open boundary conditions. We use finite-size scaling to get $\lim_{\mathcal{N}\to\infty} M^2$, see Fig. 2. We find that the scaling behavior changes from $M^2 = a + b\mathcal{L}^{-2} + \cdots$, where $\mathcal{L}^2 = \mathcal{N}$, for low electron concentrations $p = n/\mathcal{N}$ to $M^2 = a + b\mathcal{L}^{-1} + \cdots$ at higher p. In the main panel of Fig. 2 we present M^2 for finite systems as well as the extrapolated values for the most interesting region of electron concentration where ferromagnetism arises. This plot definitely demonstrates that the ferromagnetic transition point p_f is different from the standard percolation transition point $p_c = 0.5927460\ldots$ [7]. From the extrapolated data for M^2 we find a smooth transition at $p_f^M \approx 0.65$. Interestingly we also find that above p_f^M there is an extended region of *unsaturated* ferromagnetism; M^2 approaches unity very slowly with increase of p indicating that ferromagnetism remains unsaturated (e.g., M^2 is about 0.95 at $p = 0.75$). The reason for that is the distribution of configurations above p_f^M, which exhibits, in contrast to the standard percolation, together with a large cluster a quite large fraction of small clusters this way increasing the weight of the configuration [see also panel d) in Fig. 1].

An important quantity is the spanning probability $P_{\rm span}$ [7], i.e., the probability that a spanning cluster appears. Clearly, the appearance of a spanning cluster is related to the emergence of the magnetic moment. We have calculated $P_{\rm span}$ for systems up to 100×100 sites employing periodic boundary conditions, see the main panel in Fig. 3. As expected, $P_{\rm span}$ tends to zero near the percolation transition at $p_f^M \approx 0.65$ obtained from data for M^2. However, the estimate for the transition point p_f obtained from $P_{\rm span}$ is $p_f^s \approx 0.657$, slightly above p_f^M. Obviously, $P_{\rm span}$ increases from 0 to 1 as p varies in a finite region from $p \approx 0.657\ldots0.700$. That is in contrast to the standard percolation where $P_{\rm span}$ exhibits a jump between 0 and 1 at p_c.

The behavior of the normalized number of clusters around the critical region (see the inset of Fig. 3) gives another estimate for p_f which is about $p_f^n = 0.650\ldots0.665$. Slightly below this concentration the l-dependence of $n(l)$ indicates an exponential decay, slightly above this concentration $n(l)$ indicates the appearance of a large component (the second peak), whereas at the critical concentration we observe for $n(l)$ indications of a power-law decay (not shown here).

Our findings are consistent with a visual analysis of typical snapshots of configurations for the standard and weighted percolation [see panels a) - d) in Fig. 1]. Indeed for electron concentrations $p < p_f$ the system tends to form many small clusters which increase the weight. Slightly above critical concentration $p > p_f$ the large cluster is still suppressed by existence of many small clusters which help to increase the weight of configuration.

5. Conclusions and perspectives

We have consider a new correlated percolation problem which arises in a strongly correlated flat-band system, where the weights of the geometrical configurations take nontrivial values due to the Pauli principle.

The Pauli correlated problem can be examined exactly in 1D and simulated efficiently in 2D. To determine the transition point p_f of the Pauli-correlated percolation on the square lattice we use three different quantities leading to $p_f = 0.66 \pm 0.01$. From the extrapolation of finite size data we obtained a smooth transition. However, a tendency for the coexistence of a large component along with a finite fraction of smallest possible clusters could be a hint for the weak first order transition in the system.

It is important to stress here the possible experimental realizations of the flat-band ferromagnets. Recently, exact solutions have been applied to investigate f-electron ferromagnetism due to a flat band in the correlated electron material $CeRh_3B_2$ which can be mapped onto a 1D Tasaki chain [11]. Recent progress in chemistry and nanotechnology allows a fabrication of desired lattice geometries by an array of quantum dots where the number of electrons can be control by a gate voltage or by synthesizing a new materials with a desired lattice structure and intersite interactions. The systems of interest could be also constructed for cold atoms in a controlled setup of optical lattices [2]. Emerging interest in flat-band systems comes from the field of quantum Hall physics where it was shown that electronic systems with topologically non-trivial flat bands could lead to fractional quantum Hall states and fractional topological insulators in real materials (see [12] and references therein). Introducing an on-site Coulomb repulsion in the systems with topological flat bands could lead to flat-band ferromagnetism which corresponds to a quantum Hall ferromagnet [13].

Acknowledgments

The authors would like to thank J. Chalker and A. Naum for valuable discussions. M.M. thanks DAAD (A/10/84322) and DFG (SFB 602) for support of his stays in University of Göttingen and University of Magdeburg in 2010-2011 and acknowledges the kind hospitality of the host

institutions. He also thanks MPIPKS-Dresden for the kind hospitality in 2011. A.H. acknowledges support by the DFG through a Heisenberg fellowship (Project HO 2325/4-2). O.D. acknowledges the kind hospitality of University of Magdeburg in October-December of 2011.

A. Pauli-correlated percolation in one dimension

One-dimensional percolation can be analyzed using a transfer-matrix method. Introducing the partition function $Z(p,\mathcal{N})$ of a percolating system as the sum of probabilities of all possible random realizations, we can write it in terms of the transfer matrix $\mathbf{T}$ as: $Z(p,\mathcal{N}) = \mathrm{Tr}\mathbf{T}^{\mathcal{N}}$, where p is the occupation probability of a site. The transfer matrix for the Pauli-correlated percolation in one dimension, which counts the contribution of the site configurations (empty site, occupied with up-electron, occupied with down-electron) to the partition function depending on the configuration of the neighboring site, reads

$$\mathbf{T} = \begin{pmatrix} T(0,0) & T(0,\uparrow) & T(0,\downarrow) \\ T(\uparrow,0) & T(\uparrow,\uparrow) & T(\uparrow,\downarrow) \\ T(\downarrow,0) & T(\downarrow,\uparrow) & T(\downarrow,\downarrow) \end{pmatrix} = \begin{pmatrix} 1 & 1 & 1 \\ z & z & z \\ z & 0 & z \end{pmatrix}. \qquad \text{(A.1)}$$

The matrix elements $T(n_i, n_{i+1})$ correspond to the pair of neighboring sites i and $i+1$ and acquire the value 1 (z) if the site i is empty (occupied). Note that the spin configuration $T(\downarrow,\uparrow)$ is formally forbidden (whereas the spin configuration $T(\uparrow,\downarrow)$ is allowed) in order to count correctly the degeneracy of a cluster. To determine the unknown contribution z of an occupied site, we calculate the average occupation number of the site $\langle n_i\rangle$ which should be equal to p. Thus we have [9]

$$\langle n_i\rangle = \frac{\mathrm{Tr}\mathbf{T}^{\mathcal{N}}\mathbf{N}}{\mathrm{Tr}\mathbf{T}^{\mathcal{N}}} = p,\ \mathbf{N} = \begin{pmatrix} 0 & 0 & 0 \\ 0 & 1 & 0 \\ 0 & 0 & 1 \end{pmatrix}. \qquad \text{(A.2)}$$

In what follows we consider the thermodynamic limit $\mathcal{N} \to \infty$. Simple algebra leads to $z = p(2-p)/[4(1-p)^2]$. It appears that the transfer matrix for the Pauli-correlated percolation (A.1) is formally identical with that one already introduced in our previous paper [8] for counting localized hard-dimer electron states, see Eq. (A1) in Ref. [8]. However, the meaning of $\mathbf{T}$ and hence also the parameter z are different.

We turn to the calculation of the average number of clusters of size l (normalized by the lattice size $\mathcal{N}$) $n(l)$ [7]. To fix the cluster of length l we start with an empty site, then we have a string (cluster) of l occupied sites, and the last site of this string is followed by an empty one. To calculate $n(l)$ we have to replace the product of a sequence of $l+1$ $\mathbf{T}$-matrices by the product $\mathbf{SC}^{l-1}\mathbf{F}$, where

$$\mathbf{S} = \begin{pmatrix} 0 & 1 & 1 \\ 0 & 0 & 0 \\ 0 & 0 & 0 \end{pmatrix},\ \mathbf{C} = \begin{pmatrix} 0 & 0 & 0 \\ 0 & z & z \\ 0 & 0 & z \end{pmatrix},\ \mathbf{F} = \begin{pmatrix} 0 & 0 & 0 \\ z & 0 & 0 \\ z & 0 & 0 \end{pmatrix}. \qquad \text{(A.3)}$$

That yields

$$n(l) = \frac{\mathrm{Tr}\mathbf{T}^{\mathcal{N}-l-1}\mathbf{SC}^{l-1}\mathbf{F}}{\mathrm{Tr}\mathbf{T}^{\mathcal{N}}}. \qquad \text{(A.4)}$$

After straightforward calculations we arrive at

$$n(l) = \frac{4(1-p)^3}{(2-p)^2}(l+1)\alpha^l\ ,\ \alpha = \frac{p}{2-p}, \qquad \text{(A.5)}$$

see Eq. (3.1). In these calculations we have used the relation

$$\mathbf{C}^m = z^m \begin{pmatrix} 0 & 0 & 0 \\ 0 & 1 & m \\ 0 & 0 & 1 \end{pmatrix}. \qquad \text{(A.6)}$$

Next, we use the transfer-matrix approach to calculate the (pair) site-occupation correlation function $g(l) = \langle n_i n_{i+l}\rangle - \langle n_i\rangle\langle n_{i+l}\rangle = \langle n_i n_{i+l}\rangle - p^2$ [10]. Using the matrix $\mathbf{N}$ defined in Eq. (A.2) and calculating $\mathrm{Tr}\mathbf{T}^{\mathcal{N}-l}\mathbf{NT}^l\mathbf{N}$ [9] we get

$$g(l) = -(1-p)^2\alpha^{2|l|}. \qquad \text{(A.7)}$$

Finally, we calculate the pair connectivity $\Gamma(n, n+l)$ (the probability that two sites n and $n+l$ are both occupied and belong to the same cluster). For this purpose we have to consider the quantity

$$\Gamma(n, n+l) = \frac{\mathrm{Tr}(\mathbf{T}^{\mathcal{N}-l}\mathbf{NC}^l)}{\mathrm{Tr}\mathbf{T}^{\mathcal{N}}}, \qquad \text{(A.8)}$$

which after similar calculations transforms into

$$\Gamma(n, n+l) = p\cdot\left(1 + \frac{1-p}{2-p}l\right)\alpha^l. \qquad \text{(A.9)}$$

The elaborated approach can be applied to the standard percolation, too. In this case

$$\mathbf{T} = \begin{pmatrix} 1 & 1 \\ z & z \end{pmatrix},\ \mathbf{N} = \begin{pmatrix} 0 & 0 \\ 0 & 1 \end{pmatrix},$$
$$\mathbf{S} = \begin{pmatrix} 0 & 1 \\ 0 & 0 \end{pmatrix},\ \mathbf{C} = \begin{pmatrix} 0 & 0 \\ 0 & z \end{pmatrix},\ \mathbf{F} = \begin{pmatrix} 0 & 0 \\ z & 0 \end{pmatrix} \qquad \text{(A.10)}$$

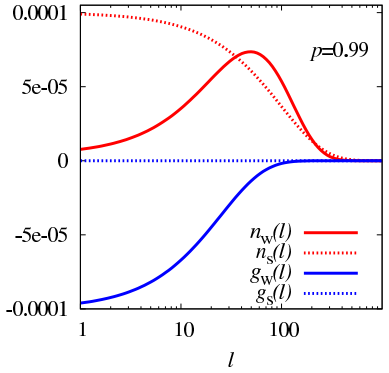

Figure 4. (Color online) $n(l)$ (red) and $g(l)$ (blue) at $p = 0.99$ for the Pauli-correlated (solid) and standard (dotted) percolations.

and formulas (A.2), (A.4), and (A.8) yield $z = p/(1-p)$, $n(l) = (1-p)^2 p^l$, $g(l) = p(1-p)\delta_{l,0}$, and $\Gamma(n, n+l) = p \cdot p^l$, respectively, see Ref. [7].

In Fig. 4 we illustrate $n(l)$ and $g(l)$ for both types of percolation at $p = 0.99$.

References

1. W. Heisenberg, Z. Phys. **38**, 411 (1926); Z. Phys. **49**, 619 (1928).
2. C. Wu, D. Bergman, L. Balents, and S. Das Sarma, Phys. Rev. Lett. **99**, 070401 (2007); E. Tang, J.-W. Mei, and X.-G. Wen, Phys. Rev. Lett. **106**, 236802 (2011); K. Sun, Z. Gu, H. Katsura, and S. Das Sarma, Phys. Rev. Lett. **106**, 236803 (2011); T. Neupert, L. Santos, C. Chamon, and C. Mudry, Phys. Rev. Lett. **106**, 236804 (2011); Y.-F. Wang, Z.-C. Gu, C.-D. Gong, and D. N. Sheng, Phys. Rev. Lett. **107**, 146803 (2011). Z. Gulácsi, A. Kampf, and D. Vollhardt, Phys. Rev. Lett. **105**, 266403 (2010); J. Schulenburg, A. Honecker, J. Schnack, J. Richter, and H.-J. Schmidt, Phys. Rev. Lett. **88**, 167207 (2002); J. Richter, O. Derzhko, and J. Schulenburg, Phys. Rev. Lett. **93**, 107206 (2004).
3. A. Mielke, J. Phys. A **24**, L73 (1991); **24**, 3311 (1991); **25**, 4335 (1992); Phys. Lett. A **174**, 443 (1993).
4. H. Tasaki, Phys. Rev. Lett. **69**, 1608 (1992); A. Mielke and H. Tasaki, Commun. Math. Phys. **158**, 341 (1993).
5. J. Hoshen and R. Kopelman, Phys. Rev. B **14**, 3438 (1976).

6. M. E. J. Newman and R. M. Ziff, Phys. Rev. E **64**, 016706 (2001).
7. D. Stauffer and A. Aharony, *Introduction to Percolation Theory* (Taylor & Francis, London, 2003).
8. O. Derzhko, A. Honecker, and J. Richter, Phys. Rev. B **76**, 220402(R) (2007); O. Derzhko, J. Richter, A. Honecker, M. Maksymenko, and R. Moessner, Phys. Rev. B **81**, 014421 (2010).
9. R. J. Baxter, *Exactly Solved Models in Statistical Mechanics* (Academic Press, London, 1982).
10. A. Weinrib, Phys. Rev. B **29**, 387 (1984).
11. Z. Gulácsi, A. Kampf, and D. Vollhardt, Prog. Theor. Phys. Suppl. 176, 1 (2008).
12. D. N. Sheng, Z.-C. Gu, K. Sun, and L. Sheng, Nat. Commun. **2:389**, 1380 (2011); K. Sun, Z. Gu, H. Katsura, and S. Das Sarma, Phys. Rev. Lett. **106**, 236803 (2011).
13. H. Katsura, I. Maruyama, A. Tanaka, and H. Tasaki, Europhysics Letters **91**, 57007 (2010).